11th Australasian Fluid Mechanics Conference
University of Tasmania, Hobart, Australia
14-18 December 1992

INTERACTION OF THE EKMAN LAYER AND SIDEWALL BOUNDARY LAYER WITH SYSTEM ROTATION AND ADVERSE PRESSURE GRADIENT

Ian MACFARLANE and P.N. JOUBERT

Dept of Mechanical & Manufacturing Engineering
University of Melbourne, Parkville, VIC 3052
AUSTRALIA

ABSTRACT

The work presented here represents a preliminary report on an investigation into the influence of secondary flows on a turbulent boundary layer developing on the side walls of a rotating diffuser. The diffuser angle and rotational speed have been selected such that full two dimensional stall is observed. The aspect-ratio of the diffuser working section is then varied to allow the secondary cross flows a greater influence on the midspan meanflow profiles and the subsequent effects to be seen. Meanflow, skin friction and pressure coefficient data are presented.

INTRODUCTION

Although there have been some reports presented on the effect of system rotation on developing turbulent boundary layers, due to the complex nature of such flows, there remains a need for good experimental data to aid our understanding in this area. The aim of the current study is to obtain reliable data for the case with adverse pressure gradient and system rotation, where the aspect-ratio of the rotating diffuser is varied to allow the secondary cross flows (or Ekman layer flows) to influence the sidewall boundary layers to a varying degree.

The Ekman layer flows are generated by an imbalance between the Coriolis force and pressure force acting on the slower moving particles at the top and bottom walls of the rotating diffuser. This imbalance deflects fluid from the pressure side toward the suction side causing the secondary flows. Some previous studies have been conducted in high and low aspect-ratio, zero pressure gradient ducts and some work has been undertaken to investigate the additional effect of adverse pressure gradient.

Rothe and Johnston (1976), from their pressure measurement work in a rotating plane wall diffuser, observed that "the dominant picture of stall in a rotating diffuser is one of steady relatively quiescent, fixed pockets of near stagnant flow."

The boundary layer development observed by Watmuff Witt and Joubert (1985) in their zero pressure gradient rotating duct was for suction side layers to be suppressed while the pressure side layers were enhanced compared with the zero rotation case. The aspect-ratio of the duct used in these experiments was 4:1 (height:width).

Ibal (1990) and Ibal and Joubert (1992) studied the effects of adverse pressure gradient and system rotation on developing turbulent boundary layers on the side wall of a rotating diffuser. The inlet aspect-ratio was 4:1 (h:w) and two pressure gradients were used corresponding to 3 and 8 degree diffusing angles (case 1 and 2 respectively). For case 1, rotation rates of 40 and 60 rpm were studied. In case 2, only the 40 rpm speed was considered. It was found for case 1 that the flow was attached throughout the working section for the lower speed, while at the higher speed pockets of corner stall were seen. The stronger adverse pressure gradient showed full two dimensional stall. Centre line boundary layer profiles showed that boundary layer growth was promoted on the pressure side and suppressed on the suction side compared with the non-rotating layers, except for the stronger adverse pressure gradient case where in the stations downstream of separation it was observed that the pressure side growth was suppressed. This was attributed to the region of separation 'squeezing' the flow, thus lowering the effective diffusion, rather than to the possible influence of secondary flows.

Hill and Moon (1962) and Moon (1964) studied the effects of system rotation on developing turbulent boundary layers on the side wall of low aspect-ratio rotating rectangular channels. The measurements showed that boundary layer growth was promoted on the suction side while suppressed on the pressure side. This is in agreement with the conclusions of the preliminary report presented by Koyama et al.(1989) who were conducting experiments in a 1:7 (h:w) aspect-ratio rotating channel. This is contrary to the findings of Watmuff et al. (1985) and Ibal (1990), working in the 4:1 (h:w) rotating channel and diffuser respectively

The explanation for the opposite trends observed in boundary layer growth mentioned above is that for the higher aspect-ratio experimental rigs, the secondary flow effects are sufficiently removed from the centre line velocity profiles as to provide negligible influence. In the lower aspect-ratios, the secondary flows are sufficiently close to the centre line profiles to overcome the Coriolis instability.

APPARATUS AND TECHNIQUES

The open return tunnel used in the experiments is shown in figure 1. Air flow was provided by a two stage axial fan located on the floor above the rotating assembly. The air passed through rotating ductwork fitted with turning vanes and honeycombs to ensure that the flow was approximately irrotational relative to the duct at the working section entry.

The working section is shown diagrammatically in figure 2 and consists of a perspex diffuser with walls hinged in the vertical plane to allow the adverse pressure gradient to be imposed. The walls were set to an 8 degree diffusing angle and the speed of rotation for the measurements was 40 rpm, corresponding to case 2 used by Ibal (1990) in which the two dimensional stall was observed. This operating condition was chosen to enable the effects of changing aspect-ratio on the separated flow region to be observed. The tunnel velocity was set to a unit Reynolds number of $Re_{ref} = 664000$ ($Re_{ref} = \frac{\rho U}{\mu}$) corresponding to a nominal velocity of 10 m/s. The boundary layers were tripped by a 1.2 mm diameter trip wire.

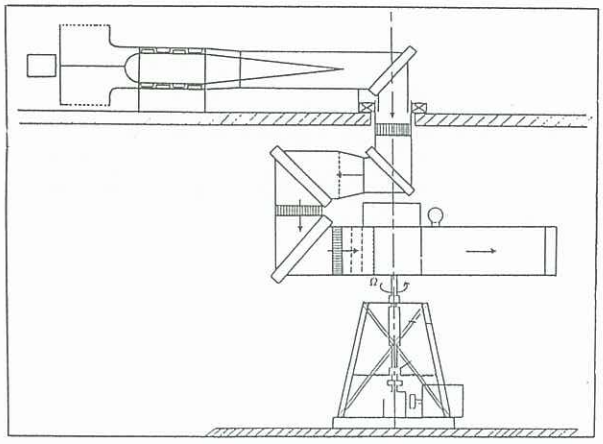

Figure 1: Elevation of rotating wind tunnel

The variable aspect-ratio was brought about by inserting a false horizontal panel which was fitted at several heights. This partitioned the working section into an upper and lower region. The lower section was free from obstructions and was used for the measurements. Measurements for inlet aspect-ratios of 1:1 and 2:1 (h:w) (*ar1* and *ar2* respectively) are presented here.

A traverse mechanism was mounted on one side of the working section. All measurements were taken on the opposite plane smooth wall. To observe the pressure and suction side walls the direction of rotation was reversible.

Signals were transferred to and from the rig by a series of slip rings, which also provided access for 240V power to supply the instrumentation mounted on the rig. Pressures were measured by differential electronic manometers mounted on the rotational axis of the rig. The manometer outputs were amplified prior to transmission through the slip rings to reduce the signal-to-noise ratio.

Control of the traverse mechanism and monitoring of the rotation rate was accomplished automatically by an Analogue Devices RTI-827 digital counter timer card installed in an Osborne 386 IBM compatible computer. Sampling of the analogue signals was by an Analogue Devices RTI-860 card mounted in the same computer. Mean values for the analogue signals were measured by digitally averaging the signals for a period of 40 seconds and then taking sufficient samples to achieve convergence within the equipment tolerance. Three samples were generally found to be sufficient.

Mean velocity profiles were obtained with a round 0.6 mm diameter total head tube using an adjacent wall pressure tapping as the static reference. For the rotating profiles, the static pressure profile was measured and the velocity readings which were calculated from the wall reference tapping were corrected accordingly. One obvious limitation of the results obtained with this method is the lack of resolution of the cross flow components of velocity, which may be significant in the centre line profiles particularly for the lower aspect-ratio. However at this stage the potential problem can only be noted. The answer will be evaluated by means of cross wire measurements at a later stage in the project.

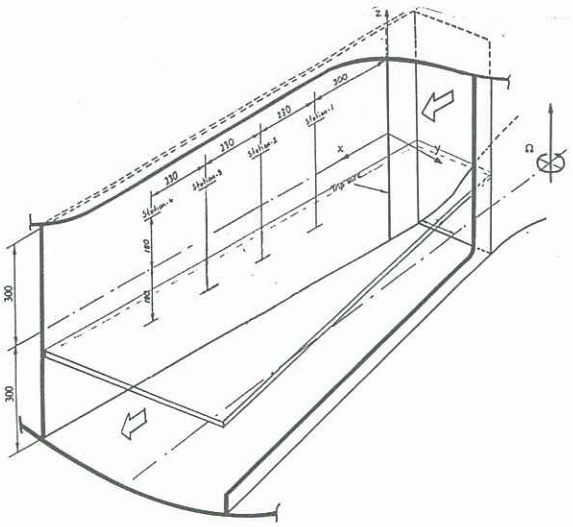

Figure 2: Schematic view of working section

Traverse backlash and deflections due to centrifugal forces were overcome by lightly pressing the probe against the wall and then moving the probe outward in 0.01 mm increments until the averaged manometer readings indicated that the probe had just left the wall. Once the wall zero reading had been established the computer automatically traversed the probe in logarithmic steps to measure the boundary layer profile.

EXPERIMENTAL RESULTS

The pressure coefficient was defined as:

$$C_p = \frac{P^* - P_i^*}{\frac{1}{2}\rho U_{ref}^2}$$

where the subscript i refers to the reference pressure tapping located at a streamwise distance of 60 mm from the trip wire. A plot of Cp verses streamwise distance x is shown in figure 3. The curves for both *ar1* and *ar2* show decreasingly adverse pressure gradient behaviour. The pressure recovery is further reduced beyond station 2 for the rotating cases compared to the non-rotating cases. This is thought to be caused by the two dimensional stall on the suction side deflecting the flow streamlines toward the pressure side thus lowering the effective diffusion downstream of the point of separation. The rotating curves for both *ar1* and *ar2* fall below the zero rotation curves between stations 2 and 3, providing no indication as to the effects of the secondary flows on the onset of stall. Beyond the point of separation, the curves show different behaviour. In the lower aspect-ratio the pressure and suction side C_p curves split after separation, while for the higher aspect ratio the curves collapse until the last measurement station. The pressure gradient for *ar1* is seen to

be shallower than for *ar2* and this is attributed to the top and bottom wall boundary layers causing proportionally larger restriction.

The skin friction measurements shown were calculated from a numerical Clauser chart method. The adverse pressure gradient results in the skin friction being reduced in the streamwise direction for the stationary cases, as shown in figure 4. Skin friction is increasing on the pressure side walls and decreasing on the suction side walls compared to the stationary case. The skin friction values for the rotating cases fall with decreasing aspect-ratio. The values for station 1 with no rotation are lower for *ar1*, but with

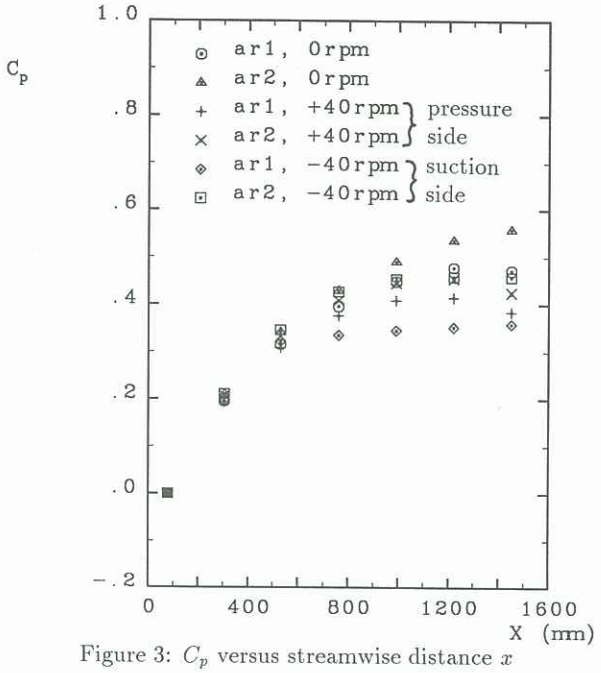

Figure 3: C_p versus streamwise distance x

streamwise distance the trend reverses until the values are slightly higher for *ar1* stations 3 and 4 compared with *ar2*.

The decreasing skin friction values for the suction side layer are regarded as an indication of the onset of stall. At station 3 the flow in the diffuser is separated on the suction side for both *ar1* and *ar2*. From this information it is impossible to ascertain whether the changing aspect-ratio has influenced the onset of stall.

Figure 5 shows the centre line mean velocity profiles developing without rotation for *ar1* and *ar2*. The logarithmic law shown in the figure is defined as:

$$\frac{U}{U_\tau} = \frac{1}{0.41} \ln \frac{yU_\tau}{\nu} + 5.0$$

The profiles appear normal for a boundary layer developing in adverse pressure gradient flow. For greater streamwise distances, the logarithmic region shortens and the wake strength parameter becomes larger. There is no sign of flow separation. It can be seen that the wake strength parameter decreases at station 4 due to the lower aspect-ratio. This is attributed to the more significant effect of the top and bottom wall boundary layers suppressing the flow as the overall diffuser area is reduced.

Figures 6 and 7 show profiles affected by rotation for station 2, *ar1* and *ar2* respectively. The logarithmic region on the pressure side wall is longer and on the suction

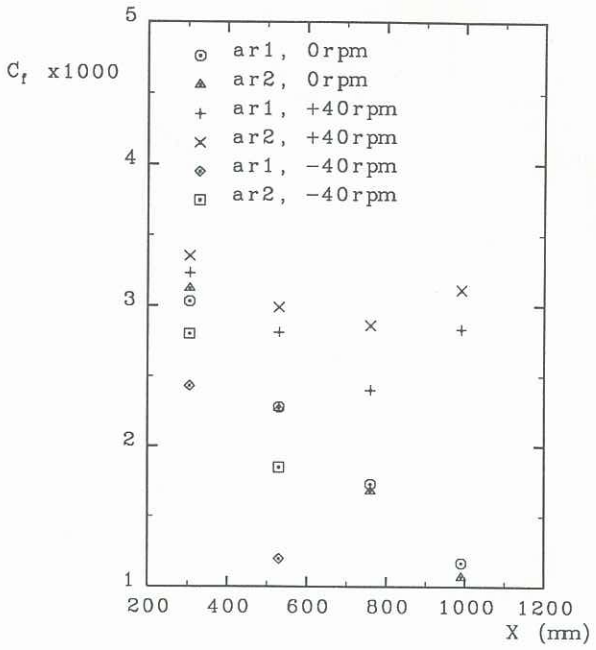

Figure 4: C_f versus streamwise distance x

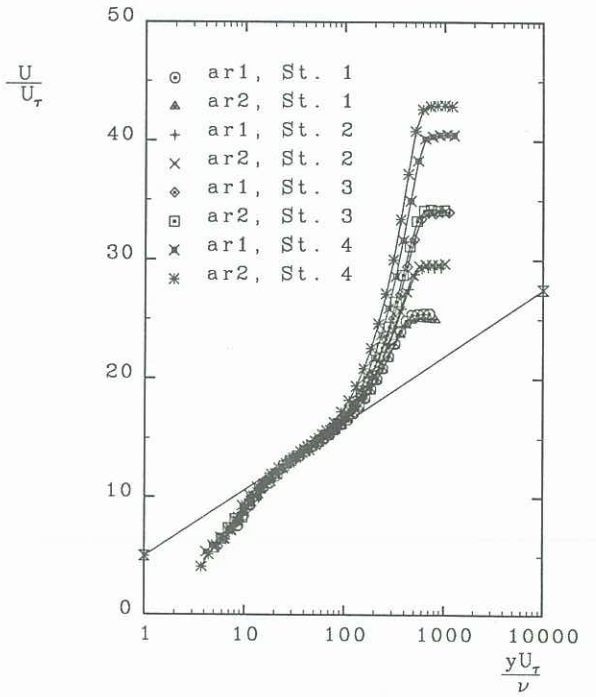

Figure 5: Stationary mean velocity profiles

side wall is shorter compared to the stationary case. The gradient of the logarithmic region for the rotating profiles also differs from the stationary case.

Some deviation from the universal inner wall region can be seen for the suction side profiles, possibly due to the onset of stall. Other than station 2 suction side, the profiles show that flow in the viscous inner region converges, indicating that this region is unaffected by system rotation. As reported by Watmuff et al. (1985), the Coriolis forces are small compared to the viscous forces in this region and as such we would expect minimal departures from the universal behaviour.

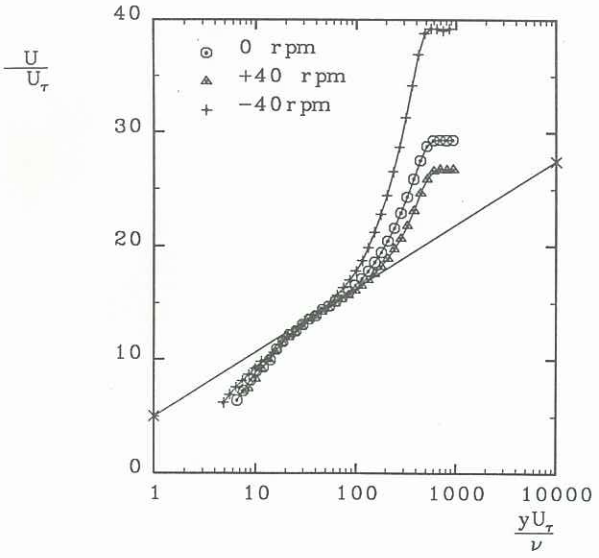

Figure 6: Station 2, *ar1* mean velocity profile

In the wake region it is observed in all cases that the wake strength parameter is increased on the suction side while for the pressure side it is decreased.

The boundary layer thickness δ_{995} is defined as the point where the mean velocity reaches 0.995 times the local free stream velocity. Boundary layer thickness with streamwise distance is shown in figure 8.

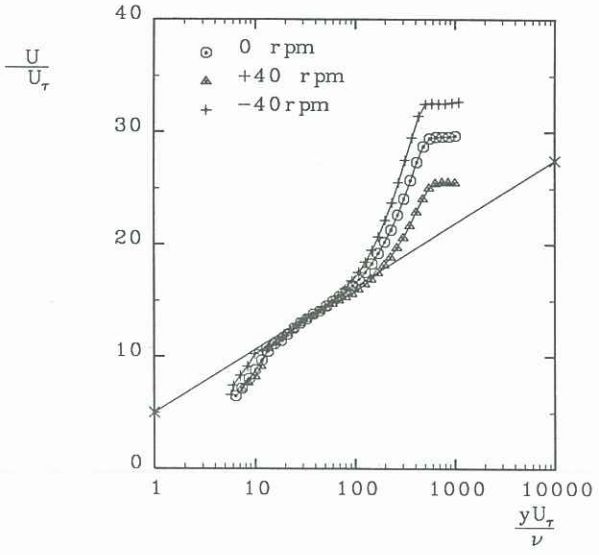

Figure 7: Station 2, *ar2* mean velocity profile

The boundary layer thickness is reduced with the lower aspect-ratio in all cases. In all instances the boundary layer growth is promoted on the suction side compared with the zero rotation case. The pressure side thickness is slightly greater for station 1, while for stations 2 to 4 the boundary layer growth is suppressed compared to the zero rotation case. At station 1 the secondary flow effects would be minor, but with streamwise distance the effects strengthen and by station 2 the pressure and suction side profile growth is consistent with that reported by previous workers in low aspect-ratio ducts.

CONCLUSIONS

It can be seen from the preliminary work reported here that for the lower aspect-ratio, with the resulting increased influence of the secondary flows on the side wall boundary layers, that the secondary flows appear to have little influence on the onset of stall. It is also observed that the boundary layer growth is promoted on the suction side and suppressed on the pressure side as would be expected when the side wall boundary layers are significantly affected by the Ekman layer flows.

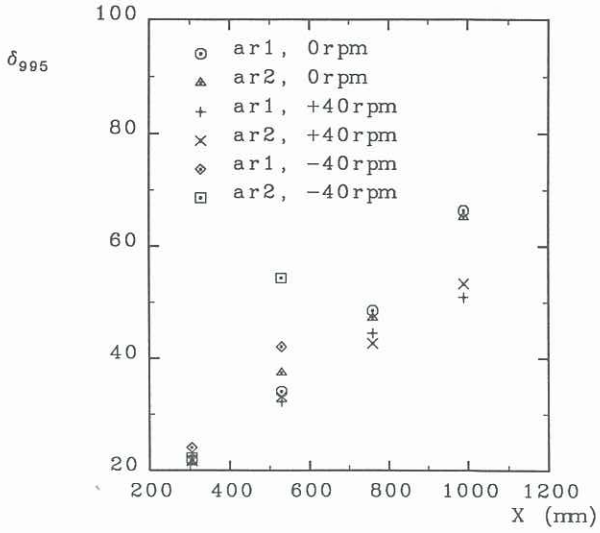

Figure 8: δ_{995} with streamwise distance x

ACKNOWLEDGMENTS

This work has been funded through the Australian Research Council and their support is gratefully acknowledged.

REFERENCES

IBAL, G. (1990) Adverse pressure gradient and separating turbulent boundary layer flows with system rotation. PhD Thesis, The University of Melbourne.

IBAL, G. and JOUBERT, P.N. (1992) A study of the combined effects of rotation and adverse pressure gradient on turbulent boundary layer flows. Part 1 meanflow results. 11th Aust. Fluid Mech. Conf., Hobart Australia.

HILL, P. G. and MOON, I. M. (1962) Effects of Coriolis forces on the turbulent boundary layer in rotating machines. Rep. No. 69, Gas Turbine Laboratory, M.I.T..

KOYOMA, H. S., TAMURA, E. and SAITO, T. (1989) Effect of Coriolis force on developing channel flow. 10th Australasian Fluid Mechanics Conference, Melbourne Australia, Dec. 11- 15.

MOON, I. M. (1964) Effects of Coriolis forces on the turbulent boundary layer in rotating fluid machines. Rep No. 74 Gas Turbine Laboratory, M.I.T..

WATMUFF, J. H., WITT, H. T. and JOUBERT, P. N. (1985) Developing turbulent boundary layers with system rotation. J. Fluid Mech., 157, pp. 405-448.